(D-(*p*-Benzoylphenylalanine)[13], Tyrosine[19])-Melanin-concentrating Hormone, a Potent Analogue for MCH Receptor Crosslinking

ROMA DROZDZ, EDITH HINTERMANN, HEIDI TANNER, URS ZUMSTEG and ALEX N. EBERLE*

Laboratory of Endocrinology, Department of Research (ZLF), University Hospital and University Children's Hospital, CH-4031 Basel, Switzerland

Abstract: A photoreactive analogue of human melanin-concentrating hormone was designed, [D-Bpa[13],Tyr[19]]-MCH, containing the D-enantiomer of photolabile *p*-benzoylphenylalanine (Bpa) in position 13 and tyrosine for radioiodination in position 19. The linear peptide was synthesized by the continuous-flow solid-phase methodology using Fmoc-strategy and PEG-PS resins, purified to homogeneity and cyclized by iodine oxidation. Radioiodination of [D-Bpa[13],Tyr[19]]-MCH at its Tyr[19] residue was carried out enzymatically using solid-phase bound glucose oxidase/lactoperoxidase, followed by purification on a reversed-phase mini-column and HPLC. Saturation binding analysis of [^{125}I]-[D-Bpa[13],Tyr[19]]-MCH with G4F-7 mouse melanoma cells gave a K_D of $2.2 \pm 0.2 \times 10^{-10}$ mol/l and a B_{max} of 1047 ± 50 receptors/cell. Competition binding analysis showed that MCH and rANF(1–28) displace [^{125}I]-[D-Bpa[13],Tyr[19]]-MCH from the MCH binding sites on G4F-7 cells whereas α-MSH has no effect. Receptor crosslinking by UV-irradiation of G4F-7 cells in the presence of [^{125}I]-[D-Bpa[13],Tyr[19]]-MCH followed by SDS-polyacrylamide gel electrophoresis and autoradiography yielded a band of 45–50 kDa. Identical crosslinked bands were also detected in B16-F1 and G4F mouse melanoma cells, in RE and D10 human melanoma cells as well as in COS-7 cells. Weak staining was found in rat PC12 phaeochromocytoma and Chinese hamster ovary cells. No crosslinking was detected in human MP fibroblasts. These data demonstrate that [^{125}I]-[D-Bpa[13],Tyr[19]]-MCH is a versatile photocrosslinking analogue of MCH suitable to identify MCH receptors in different cells and tissues; the MCH receptor in these cells appears to have the size of a G protein-coupled receptor, most likely with a varying degree of glycosylation. Copyright © 1999 European Peptide Society and John Wiley & Sons, Ltd.

Keywords: melanin-concentrating hormone; peptide synthesis; photocrosslinking; MCH receptor; receptor analysis

* Correspondence to: Department of Research (ZLF), University Hospital, Hebelstrasse 20, CH-4031 Basel, Switzerland.

INTRODUCTION

The heptadecapeptide melanin-concentrating hormone (MCH) was originally isolated from teleost fish where it induces pigment aggregation [1,2]. In mammals, MCH was found to be a nonadecapeptide cyclized by a disulphide bridge between Cys[7] and Cys[6] (Figure 1) [3,4]. Although abundant MCH-containing cell bodies have been localized in the lateral and posterior hypothalamus of the mammalian brain, in regions commonly believed to be involved with motivational behaviours associated with arousal, eating and drinking [5], the physiological role of MCH in the mammal is not yet clear. Injection of MCH into the lateral ventricles of the rat

brain stimulates food intake in experimental animals [6,7]. As this effect of MCH can be antagonized by α-MSH, neurotensin and GLP-1 [8], there seems to be a functional interaction of MCH with anorectic neuropeptides. In addition, MCH may also interact with other orexigenic neuropeptides such as NPY [8] where the MCH effect is thought to be associated with downstream signalling of NPY-induced feeding behaviour [9].

The analysis of receptors for MCH is crucial for the identification of the sites of action of this peptide in the mammalian brain. The recent development of [^{125}I]-[Phe^{13},Tyr^{19}]-MCH as biologically active radioligand [10] was an important step forward in the determination and characterization of MCH receptors in different cell lines [11]. Yet, as MCH receptor cDNA is not available to date, additional means for the analysis of MCH receptors are required such as photocrosslinking of MCH-receptor-ligand systems. This methodology has become a powerful tool for the biochemical characterization of many receptor systems and for the study of receptor subtypes, e.g. for α-MSH [12–14], insulin [15], NPY [16], PACAP [17] and angiotensin [18].

In the present study, we describe the synthesis and application to receptor crosslinking of a photoreactive analogue of MCH, [D-Bpa^{13},Tyr^{19}]-MCH (Figure 1). The structure of this analogue was based on that of [Phe^{13},Tyr^{19}]-MCH [10] in which the tyrosine residue had been shifted from position 13 to position 19 because radioiodine at position 13 had been shown to strongly diminish the biological activity of MCH. When incorporated at position 19, the biological characteristics of MCH were not altered by the radioiodine [11]. As a photolabile residue, the D-enantiomer of p-benzoylphenylalanine (D-Bpa) was chosen and placed in the centre of the MCH molecule, thus replacing the Tyr^{13}/Phe^{13} residue which is thought to interact closely with the receptor [11].

MATERIALS AND METHODS

Chemicals and Reagents

Solvents, coupling reagents and PEG-PS resin were obtained from Milligen (Milford, MA, USA) and protected amino acid derivatives from Bachem (Bubendorf, Switzerland) or Calbiochem-Novabiochem (Läufelfingen, Switzerland). Iodine (puriss.) was purchased from Fluka (Buchs, Switzerland). RP-HPLC was carried out on a PC-controlled Jasco instrument consisting of two PU-980 pumps, a 970/975 UV/VIS detector, an 851 AS autosampler and ICL 6000 software. For semipreparative HPLC, Vydac C_{18} columns (1.0×25 cm; 5 μm granulometry; 300 Å porosity) were run with 3 ml/min of eluent A (0.1% TFA/H_2O) and eluent B (70% acetonitrile/0.1% TFA/H_2O) forming a gradient from 15 to 70% B within 40 min (monitoring at 280 nm). Analytical HPLC was performed on Vydac C_{18} columns (0.46×25 cm) at a flow rate of 1 ml/min. Amino acid analyses were performed in our laboratory on a Waters instrument using the PicoTag method. Mass spectrometry analysis was performed on a Linear Scientific 1700 MALDI system (Reno, NV, USA) at Novartis Pharma Ltd (Basel, Switzerland).

Peptide Synthesis

Linear [D-Bpa^{13},Tyr^{19}]-MCH was synthesized on a Milligen 9050 automated peptide synthesizer using the continuous-flow technology [19,20] with 1.0 g Fmoc-Tyr(tBu)-PEG-PS resin and the acid-labile hydroxymethylphenoxyacetyl linker (HMPA) [19]. The substitution of the resin was 0.15–0.2 meq/g. The following sequence of operations was used: (1) flow of 20% piperidine/DMF (7 min; cleavage of Fmoc); (2) flow of DMF (5 min; wash); (3) recirculation of Fmoc-amino acid residue (acylation; times see below); (4) flow of DMF (10 min; wash). Coupling reactions were carried out with a 4-fold excess of

H-Asp-Phe-Asp-Met-Leu-Arg-Cys-Met-Leu-Gly-Arg-Val-Tyr-Arg-Pro-Cys-Trp-Gln-Val-OH   *a*

H-Asp-Phe-Asp-Met-Leu-Arg-Cys-Met-Leu-Gly-Arg-Val-*D*-Bpa-Arg-Pro-Cys-Trp-Gln-Tyr-OH   *b*

H-Asp-Phe-Asp-Met-Leu-Arg-Cys-Met-Leu-Gly-Arg-Val-*D*-Bpa-Arg-Pro-Cys-Trp-Gln-Tyr-OH   *c*
^{125}I
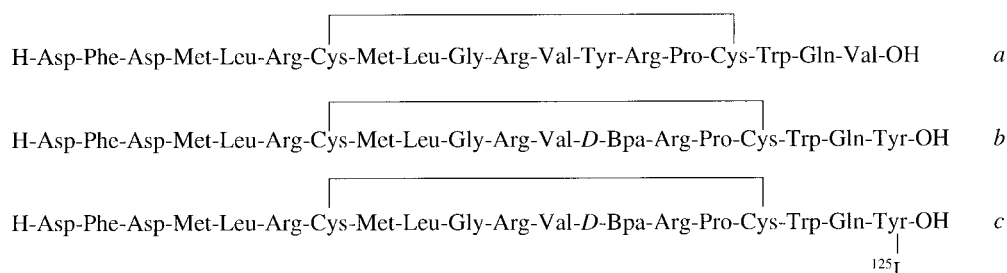
Figure 1 Structure of different forms of MCH: (a) mammalian MCH; (b) [D-Bpa^{13},Tyr^{19}]-MCH; and (c) [^{125}I]-[D-Bpa^{13},Tyr^{19}]-MCH.

protected amino acid residues, a 4-fold excess of DIPC and HOBt and the following acylation times: Fmoc-Gln(Trt)-OH (45 min), Fmoc-Trp(Boc)-OH (45 min), Fmoc-Cys(Trt)-OH (45 min), Fmoc-Pro-OH (30 min, followed by re-acylation under identical conditions), Fmoc-Arg(Pmc)-OH (45 min), Fmoc-D-Bpa-OH (45 min), Fmoc-Val-OH (30 min, followed by re-acylation under identical conditions), Fmoc-Gly-OH (45 min), Fmoc-Leu-OH (45 min), Fmoc-Met-OH (60 min), Fmoc-Asp(tBu)-OH (45 min). After completion of the synthesis, the N-terminal Fmoc group was cleaved with 20% piperidine/DMF, the resin was washed with DMF and ether and then dried *in vacuo*. Samples of the resin were taken for amino acid analysis before and after cleavage of the peptide. The protected peptide-resin was treated with TFA/H_2O/EDT/thioanisol 85:5:5:5 for 2 h at room temperature. The crude peptide was partitioned between 20% AcOH and DCM and the aqueous layer was washed further with DCM and cold ether. The ether extracts were back-washed with water and the combined aqueous solutions lyophilized. The peptide was examined by analytical RP-HPLC and purified by semipreparative RP-HPLC. Cyclization of the free cysteinyl groups of linear [D-Bpa[13],Tyr[19]]-MCH was achieved by iodine oxidation [21] using a 40-fold excess of iodine as previously described for [Phe[13],Tyr[19]]-MCH [10]. The peptide was again purified by RP-HPLC and then analysed by mass spectrometry and amino acid analysis.

Radioiodination

The radioiodination of [D-Bpa[13],Tyr[19]]-MCH was carried out as originally described for MSH peptides [22]. Both [D-Bpa[13],Tyr[19]]-MCH (18 μg in 9 μl of 2% acetic acid) and 50 μl of 0.3 M sodium phosphate buffer, pH 7.4, were transferred to an Eppendorf tube, to which 2.7 μl (37 MBq, 1 mCi) of Na[125]I (NEN Life Science Products, Boston, MA, USA) and 50 μl of Enzymobeads consisting of solid-phase bound glucose oxidase and lactoperoxidase (BioRad, Richmond, CA, USA) were added. The reaction was started by the addition of 20 μl + 20 μl of 1% β-D-glucose solution in water. After incubation for 1 h at room temperature, the reaction was stopped by the addition of 20 μl saturated ascorbic acid in water, followed by 0.5 ml of a 50 mM sodium phosphate solution, pH 7.4, containing 0.25% BSA and 0.02 M DTT. The tube was centrifuged at maximum speed for 3 min and the supernatant was applied to a reversed-phase mini-column, i.e. a 1-ml Mobicol (MoBiTec, Göttingen, Germany) packed with 0.3 g

Spherisorb ODS/10 μm RP-silica (Phase Separation Inc., Norwark, CT, USA). The column was washed three times with 0.8 ml of 0.3 M sodium phosphate buffer, pH 7.4, to remove unbound iodine. Monoiodinated [^{125}I]-[D-Bpa[13],Tyr[19]]-MCH was eluted in 0.8-ml fractions at 67–68% methanol using a stepwise gradient (30–70%) of methanol/1% TFA diluted with aqueous 1% TFA, and stored at −20°C. The radiopeptide was further purified by analytical HPLC, mixed with 200 μl BSA/lactose in water (4 mg/ml) and lyophilized overnight. The tracer was stored at −70°C until further use.

Fish Melanophore Assay

The biological activity of [D-Bpa[13],Tyr[19]]-MCH was determined with the microscopic melanophore assay using scales from the Chinese grass carp, *Ctenopharyngodon idellus*, as described by Baker *et al.* [23]. Human/rat MCH and sMCH served as standards.

Cell Binding Assay

Binding assays and photocrosslinking experiments were carried out with the following melanoma cells: mouse B16-F1, G4F (originating from B16 and not expressing melanocortin receptors [24]), G4F-7 (G4F cells with transfected human MSH receptor [25]) as well as human RE cells (isolated in our laboratory from a metastasis). In addition, rat PC12 phaeochromocytoma cells, COS-7 cells, CHO cells and human fibroblasts were used.

The cells were grown in modified Eagle's medium (MEM) with Earle's salt (Gibco, Paisley, UK), supplemented with 10% heat-inactivated foetal calf serum (Amimed, Basel, Switzerland), 2 mM L-glutamine, 1% MEM non-essential amino acids (100 × ; Gibco), penicillin (50 units/ml) and streptomycin (50 μg/ml), using Falcon 75 and 175 cm^2 tissue culture flasks at 37°C in a humidified atmosphere of 95% air and 5% CO_2. The cells were detached with 0.02% EDTA in phosphate buffered saline (8 g NaCl, 0.2 g KCl, 0.2 g KH_2PO_4, 1.44 g $Na_2HPO_4 \times 2H_2O$ per litre). Cell numbers were determined in a haemocytometer.

The binding medium consisted of MEM with Earle's salts containing 25 mM HEPES, 0.2% BSA, 0.3 mM 1,10-phenanthroline (Merck, Darmstadt) and 0.16 mM PMSF. The binding reaction was started by adding 0.5 ml of a cell suspension (0.5–2 × 10^6 cells/ml) to 12 × 75 mm polypropylene tubes containing: (1) 50 μl containing 0.05 pmol (200000 cpm) of [^{125}I]-[D-Bpa[13],Tyr[19]]-MCH and 50 μl of un-

labelled peptide in a 1:3 dilution series ($\rightarrow$ competition binding experiment); or (2) 50 μl containing 0.005–0.25 pmol (20000–1000000 cpm) of [^{125}I]-[D-Bpa^{13},Tyr^{19}]-MCH and 50 μl of 0.6 μM unlabelled MCH or buffer ($\rightarrow$ saturation binding experiment). The cells were incubated for 90 min at 10°C. Unbound radioactivity was removed by centrifugation of triplicate aliquots (150 μl) through a layer of 150 μl silicon oil in 0.4 ml polyethylene microtubes [26]. The oil was made up to a density of 1013 kg/cm^3 by mixing equal volumes of AR-20 and AR-200 silicon oil (Wacker Chemie, Munich, Germany). The radioactivity was counted in an Packard Riastar γ-counter and the binding data were analysed with Ligand, an iterative non-linear regression program established for Mac personal computers [27].

Photoaffinity Labelling

Live cells (2.5–5×10^6) were suspended in binding buffer (50 m\M Tris–HCl, pH 7.4, containing 1.4 m\M CaCl$_2$, 109 m\M NaCl, 9.8 m\M MgCl$_2$, 5.4 m\M KCl, 0.3 m\M 1,10-phenanthroline and 0.16 m\M PMSF) and incubated in polypropylene tubes at 10°C together with 100 μl of 0.9 n\M [^{125}I]-[D-Bpa^{13},Tyr^{19}]-MCH in the presence or absence of 1 μM MCH. After 90 min of incubation, the cells were UV-irradiated on ice for 5 min, 10 min, 20 min, 40 min or 1 h, using the > 310 nm spectrum of a 1-kW Oriel mercury–xenon UV-lamp [28]. Irradiated cells were washed extensively with cold 0.2% EDTA/PBS and PBS, centrifuged at 13000 g for 10 min and the pellets resuspended in 10 m\M Tris–HCl, pH 7.4, containing 1 m\M 1,10-phenanthroline and again centrifuged. Finally, the cells were resuspended in lysis buffer (2 m\M Tris–HCl, pH 7.4, containing 1 m\M 1,10-phenanthroline and kept at -20°C overnight. The frozen cells were rapidly thawed at 37°C and homogenized. The lysed cells were centrifuged at 10000 g and benzoase (75 units/sample) was added. The cells were kept at 37°C for 30 min, centrifuged at 10000 g for 5 min, washed with PBS and again centrifuged. The pellets were resuspended in SDS-PAGE sample buffer (2% SDS, 62.5 m\M Tris–HCl, pH 6.8, 10% glycerol, 5% β-mercaptoethanol and 0.001% bromophenol blue) and subjected to SDS-PAGE using 10% polyacrylamide gels. The gels were stained with 0.25% Comassie blue R250 in 1% acetic acid/45% methanol for 10 min, destained, dried and exposed to a Kodak X-Omat S film at -70°C.

RESULTS

Synthesis of (D-Bpa^{13},Tyr^{19})-MCH

The continuous-flow solid-phase synthesis of linear [D-Bpa^{13},Tyr^{19}]-MCH (Figure 1) was carried out on PEG-PS resin (0.15–0.2 meq/g) containing polyethyleneglycol spacers grafted on a gel-type support which were then derivatized to amino functions and consecutively enlarged with HMPA linker and Fmoc-Tyr(tBu)-OH. Thiol groups of Cys were protected with Trt. The assembly of the peptide was performed with a 4-fold excess of individual residues in conjunction with relative short coupling times. The acylation with Fmoc-Pro-OH and Fmoc-Val-OH (steps 6 and 8) was repeated once. Linear [D-Bpa^{13},Tyr^{19}]-MCH with free -SH groups was obtained through a 2 h cleavage in TFA (85%) containing EDT (5%) and thioanisol (5%) as scavengers as well as water (5%), followed by HPLC purification. The yield of the final product was only 50% but in good quality. Oxidation of the linear [D-Bpa^{13},Tyr^{19}]-MCH was performed with iodine: cyclic [D-Bpa^{13},Tyr^{19}]-MCH was obtained in 38% yield after Sephadex G-25 chromatography and in 28% yield after HPLC purification. MALDI mass spectrometry revealed a protonated monoisotopic ion at 2541.9 amu (calculated mH$^+$ 2541 amu for C$_{116}$H$_{166}$N$_{30}$O$_{27}$S$_4$). Amino acid analysis: Asp (2) 2.0; Phe (1) 1.0; Met (2) 1.7; Leu (2) 2.0; Arg (3) 3.3; Cys (2) 0.7; Gly (1) 1.0; Val (1) 0.7; Tyr (1) 1.0; Pro (1) 1.0; Trp (1) 0.1; Gln (1) 1.1; Bpa was not determined. UV-spectrophotometric analysis of the peptide ($\lambda_{max} = 262$ nm; $\varepsilon = 18000$) demonstrated that the Bpa residue had remained intact throughout the synthesis and purification steps.

Radioiodination of (D-Bpa^{13},Tyr^{19})-MCH

The solid-phase coupled glucose oxidase/lactoperoxidase method (Enzymobeads) for gentle oxidation of iodine was used, as originally developed for α-MSH [22], in order to minimize oxidation of the sulphides of Met^4 and Met^8 during radioiodination. The iodination of [D-Bpa^{13},Tyr^{19}]-MCH) required a longer reaction time (60 min) than for α-MSH and the addition of a lower amount (20 m\M) of DTT when the reaction was terminated. Immediate purification of the tracer on the RP-mini-column after the reaction and in addition, preceding each biological assay, by HPLC produced a homogeneous [^{125}I]-[D-Bpa^{13},Tyr^{19}]-MCH radioligand with approximately 2000 Ci/mmol (Figure 2).
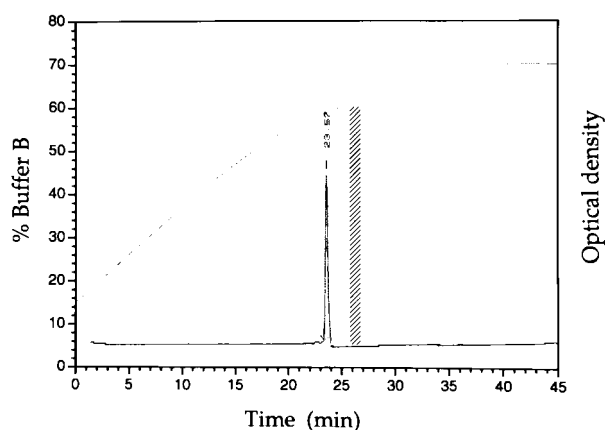
Figure 2 Analytical RP-HPLC of [D-Bpa^{13},Tyr^{19}]-MCH (retention time: 23.5 min) and elution of [^{125}I]-[D-Bpa^{13},Tyr^{19}]-MCH (hatched area; retention time: 26.3 min). Conditions of chromatography are described in 'Materials and Methods'.

Receptor Binding of (D-Bpa^{13},Tyr^{19})-MCH

Saturation and competition binding analysis of [^{125}I]-[D-Bpa^{13},Tyr^{19}]-MCH were carried out with G4F-7 cells. Association and dissociation kinetics did not differ from those determined for [^{125}I]-[Phe^{13},Tyr^{19}]-MCH [11] and are therefore not shown. Scatchard analysis of saturation binding experiments using increasing concentrations (0.2–1.2 nM) of [^{125}I]-[D-Bpa^{13},Tyr^{19}]-MCH produced a linear curve (Figure 3) from which the following dissociation constant and receptor number were calculated: $K_D = 2.2 \pm 0.2 \times 10^{-10}$ mol/l and $B_{max} = 1047 \pm 50$ sites/cell. The results of the competition binding experiments with G4F-7 cells, [^{125}I]-[D-Bpa^{13},Tyr^{19}]-MCH radioligand and MCH, α-MSH and rANF(1–28) as competitors are shown in Figure 4. The data are very similar to those obtained previously with [^{125}I]-[Phe^{13},Tyr^{19}]-MCH [11], indicating that there is virtually no difference between the two radioligands.

The biological activity of [D-Bpa^{13},Tyr^{19}]-MCH in the fish melanophore assay gave an EC$_{50}$ of about 2×10^{-10} M, which corresponds to about 50% of that of mammalian MCH.

Photocrosslinking of MCH Receptors

The time-course of UV-induced crosslinking of MCH receptors on G4F-7 cells with [^{125}I]-[D-Bpa^{13},Tyr^{19}]-MCH is demonstrated in Figure 5: The intensity of the labelled band at 45–50 kDa increased with increasing irradiation times from 5 to 20 min. No

difference could be observed between 20 or 40 min irradiation times. However, a longer irradiation time such as 60 min showed a somewhat lesser incorporation, possibly due to loss of radioiodine from the [^{125}I]-[DBpa^{13},Tyr^{19}]-MCH molecule after prolonged UV-irradiation. Figure 5 also shows that photo-incorporation of [^{125}I]-[D-Bpa^{13},Tyr^{19}]-MCH can be blocked completely by excess of cold MCH. Furthermore, no non-specific labelling of other proteins was detected.

The specificity of UV-crosslinking of [^{125}I]-[D-Bpa^{13},Tyr^{19}]-MCH to MCH receptors on G4F-7 cells was analysed by displacing the radioligand with MCH, α-MSH and rANF(1–28) before UV-irradiation (Figure 6). Both MCH and non-radioactive [D-Bpa^{13},Tyr^{19}]-MCH led to complete displacement of the photoreactive radioligand from the receptor and hence no labelled band could be detected. α-MSH did not lead to noticeable displacement whereas rANF(1–28) and sMCH showed partial displacement. No incorporation of [^{125}I]-[D-Bpa^{13},Tyr^{19}]MCH was found when the UV-irradiation step was omitted.

The occurrence of MCH receptors on cell lines different from G4F-7 cells was tested in the same way by UV-crosslinking of [^{125}I]-[D-Bpa^{13},Tyr^{19}]-MCH in the absence and presence of non-radioac-
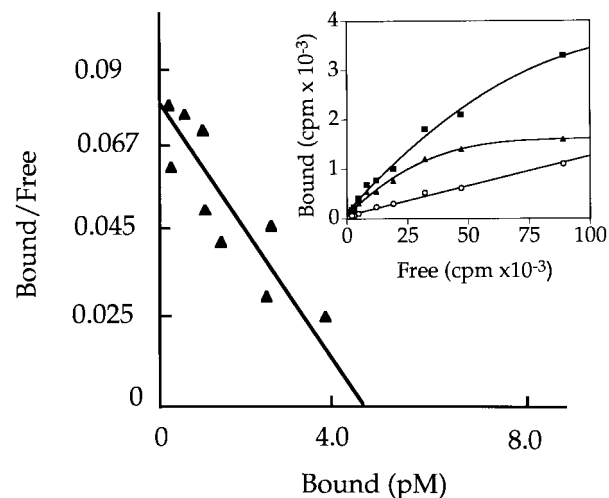

Figure 3 Scatchard analysis of a typical saturation binding experiment (insert) using G4F-7 cells and 0.005–0.25 pmol [^{125}I]-[Phe^{13},Tyr^{19}]-MCH tracer alone (→total binding; ■) or in the presence of 0.7 μM MCH (→non-specific binding; ○). The main curve represents the Scatchard transformation of specific binding data points (▼), i.e. the difference between total and non-specific binding. K_D $2.2 \pm 0.2 \times 10^{-10}$ mol/l; $B_{max} = 1047 \pm 50$ sites/cell.
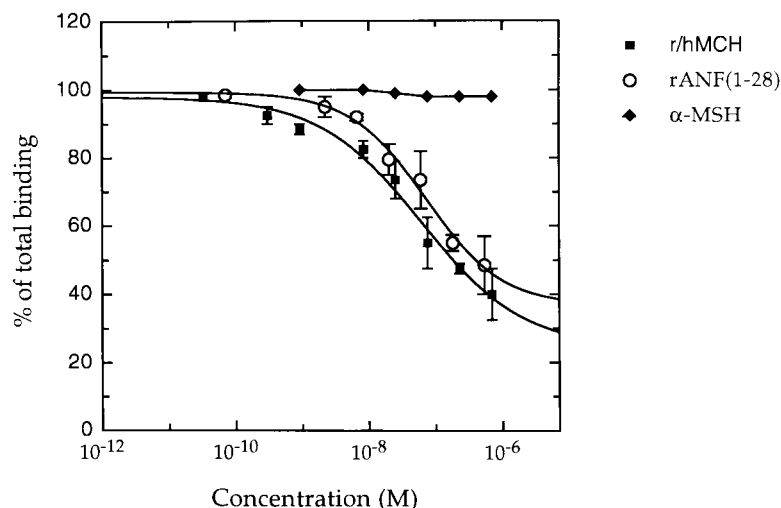
Figure 4 Log dose–response curve of human MCH (■), rANF(1–28) (○) and α-MSH (◆) in a competition binding assay with G4F-7 cells and [^{125}I]-[D-Bpa^{13},Tyr^{19}]-MCH as radioligand. The results are the mean $\pm$ S.E.M. of three independent experiments.

tive MCH (Figure 7). Whereas mouse melanoma cells (B16-F1, G4F and G4F-7) and human D10 melanoma cells (not displayed) showed intensive staining of the 45–50 kDa band only, human RE melanoma cells also showed non-specific incorporation of [^{125}I]-[D-Bpa^{13},Tyr^{19}]MCH into other bands. In COS-7 cells, the 45–50 kDa band was also labelled predominantly whereas in CHO cells incorporation was very faint. In PC12 cells, weak labelling was found at 45–50 kDa and somewhat more intensive labelling at approximately 70 kDa. No labelling was found in human MP fibroblasts.

DISCUSSION

This paper describes the first synthesis and application of a photoreactive MCH analogue for MCH receptor crosslinking. The substitution of the Tyr^{13}/ Phe^{13} residue of MCH or, respectively, [Phe^{13},Tyr^{19}]-MCH by D-Bpa resulted in a peptide with characteristics almost identical to that of MCH or [Phe^{13},Tyr^{19}]-MCH, except for the slightly higher lipophilicity and hence retarded elution in RP-HPLC. Most interestingly, the presence of the *p*-benzoyl group on the phenyl ring at position 13 of MCH hardly affected its bioactivity or binding properties, in contrast to an iodine in Tyr^{13} of natural MCH which considerably diminishes the bioactivity of the peptide and leads to a poor radioligand. The binding characteristics of [^{125}I]-[DBpa^{13},Tyr^{19}]-MCH hardly differed from those of [^{125}I]-[Phe^{13},Tyr^{19}]-

MCH reported previously [10] in both saturation and competition binding analysis. This means that D-Bpa in position 13 is well tolerated by peripheral MCH receptors.

The reason to use Bpa instead of other photoreactive amino acid residues such as *p*-azidophenylalanine (Pap) or 4′-(3-trifluoromethyl)-3H-diazirine-3-yl-phenylalanine ({Tdm}Phe) is our observation that, for example, the synthesis of [Pap^{13},Tyr^{19}]-MCH led to inhomogeneous products, possibly caused by partial destruction of the Pap residue during cyclization of the MCH molecule. The replacement of Pap by Bpa also had practical advantages in that this residue is much more stable to normal daylight and no special precautions during synthesis have to be taken. The only difference to Pap or (Tmd)Phe is that Bpa has to be UV-irradiated for a longer time period in order to obtain quantitative crosslinking. The Bpa residue has been used in many examples since its introduction as amino acid in 1987 [29], for example for the crosslinking of receptors for substance P [30], ANF [31], insulin [32], bradykinin [33], angiotensin II [34] and parathyroid hormone [35]. The D-enantiomer of Bpa was chosen here in order to obtain a topological surface around position 13 in the [D-Bpa^{13},Tyr^{19}]MCH molecule which clearly differs from that of [L-(3′-iodine)Tyr^{13}]-MCH which (as stated above) is a very weak agonist. The high potency determined for D-Bpa^{13},Tyr^{19}]-MCH supports the assumption of a topological difference between the receptor-bound state of the two analogues.
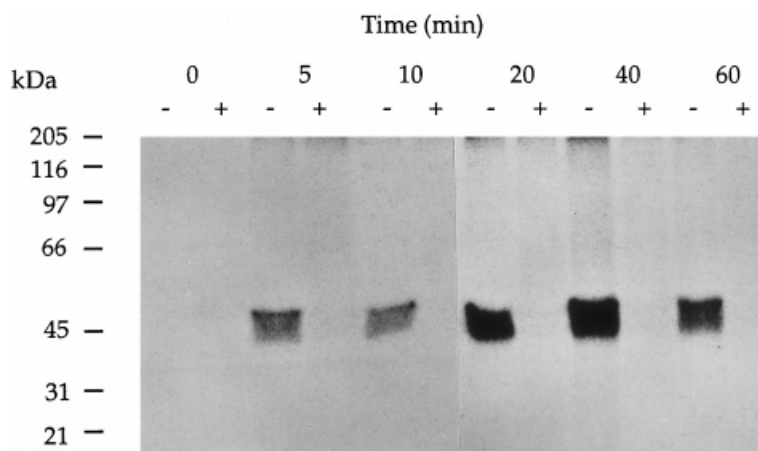
Time (min)

Figure 5 Time-course of covalent photolabelling with $[^{125}I]$-[D-Bpa^{13},Tyr^{19}]-MCH. 5×10^6 G4F-7 cells were incubated with approximately 0.6 nM $[^{125}I]$-[D-Bpa^{13},Tyr^{19}]-MCH in the absence ($-$) or presence ($+$) of 1 µM MCH in the dark at 10°C for 90 min. The samples were then exposed to UV-irradiation for varying times, washed and resuspended in SDS-PAGE sample buffer. Each lane of the SDS polyacrylamide gel was loaded with the equivalent of 2×10^6 cells. Radioactive bands were detected by autoradiography. The following protein standards were used: rabbit skeletal muscle myosin (205 kDa); *E. coli* β-galactosidase (116 kDa); rabbit muscle phosphorylase b (97.4 kDa); BSA (66.2 kDa); hen egg white ovalbumin (45 kDa); bovine carbonic anhydrase (31 kDa); soybean trypsin inhibitor (21.5 kDa).

Photocrosslinking of $[^{125}I]$-[D-Bpa^{13},Tyr^{19}]-MCH with MCH receptors on mouse G4F melanoma cells, which lack the melanocortin-1 (MSH) receptor, or on G4F-7 cells, which express the human melanocortin-1 receptor, showed a broad labelled band of 45–50 kDa which clearly differs in size and p*I* from the melanocortin-1 receptor (unpublished data). The broad band of 45–50 kDa was partly induced by the type of polyacrylamide gel used and partly by the presence of many different subpools of MCH receptor with varying degree of glycosylation, as observed for many other G protein-coupled receptors when crosslinked or analysed by Western blotting. The specificity of the UV-crosslinking using other ligands such as α-MSH, sMCH and rANF(1–28) showed that both sMCH and rANF(1–28) are weaker competitors than human MCH whereas α-MSH cannot displace [D-Bpa^{13},Tyr^{19}]-MCH from its receptor.

The previous discovery of MCH receptors on mouse and human melanoma cell lines as well as on COS-7 cells and rat P12 phaeochromocytoma cells [11] prompted us to test the $[^{125}I]$-[D-Bpa^{13},Tyr^{19}]-MCH photoligand in all these cells and a few others. Not surprisingly, labelled MCH receptor bands were found in all those cell lines in which MCH receptors had been discovered previously by binding analysis. Except for one human melanoma cell line where several membrane proteins were non-specifically labelled by $[^{125}I]$-[D-

Bpa^{13},Tyr^{19}]MCH, the labelling was always confined to the 45–50 kDa band, indicating a high degree of size-similarity of MCH receptor in different cell lines and tissues. One notable exception are PC12 cells where an additional band at around 60 kDa was also labelled. rANF(1–28) protected this band from labelling with $[^{125}I]$-[D-Bpa^{13},Tyr^{19}]-MCH whereas MCH protected both the 45–50 kDa band and the 60 kDa band. The 60 kDa band most likely corre-

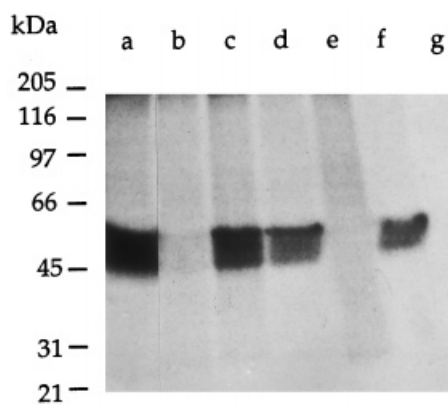Figure 6 Specificity of displacing ligands during photolabelling with $[^{125}I]$-[D-Bpa^{13},Tyr^{19}]-MCH. The experiment was performed as described in Figure 5. The following competitors were present in 1 µM concentration: (a) saline; (b) MCH; (c) α-MSH; (d) rANF(1–28); (e) [D-Bpa^{13},Tyr^{19}]-MCH; (f) sMCH; (g) saline, but no UV-light applied.
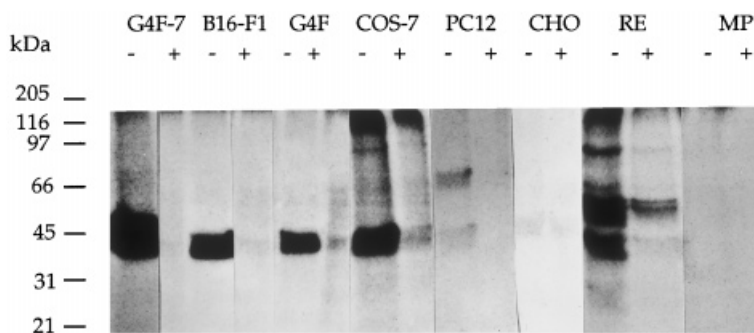
Figure 7 Photoaffinity labelling of different cell lines with [^{125}I]-[D-Bpa^{13},Tyr^{19}]MCH. Covalent labelling was achieved by incubating 5×10^6 cells with 0.9 nM [^{125}I]-[D-Bpa^{13},Tyr^{19}]-MCH in the absence ($-$) or presence ($+$) of 0.7 μM MCH. Labelled cell extracts were analysed by SDS-PAGE and autoradiography. Mouse melanoma cell lines: G4F-7, B16-F1, G4F; human melanoma cell line: RE; monkey kidney cells: CDS-7; Chinese hamster ovary cells: CHO; rat phaeochromocytoma: PC12; human fibroblasts: MP.

sponds to the 60-kDa form of one of the ANF receptors [36].

In summary, our data demonstrate that [^{125}I]-[D-Bpa^{13},Tyr^{19}]-MCH is a versatile photoreactive MCH radioligand for the identification of MCH receptors on different cell lines and tissues.

Acknowledgements

This paper is dedicated to Professor Conrad Schneider, Bern, on the occasion of his retirement as Editor-in-Chief.

REFERENCES

1. Kawauchi H, Kawazoe I, Tsubokawa M, Kishida M, Baker BI. Characterization of melanin concentrating hormone in chum salmon pituitaries. *Nature* 1983; **305**: 321–323

2. Baker BI. Melanin-concentrating hormone: a general vertebrate neuropeptide. *Int Rev Cytol* 1991; **12b**: 1–47.

3. Vaughan JM, Fischer WH, Hoeger C, Rivier J, Vale W. Characterization of melanin-concentrating hormone from rat hypothalamus. *Endocrinology* 1989; **125**: 1660–1665.

4. Nahon JL. The melanin-concentrating hormone: from the peptide to the gene. *Crit Rev Neurobiol* 1994; **8**: 221–262.

5. Bittencourt JC, Elias CF. Diencephalic origins of melanin-concentrating hormone immunoreactive projections to medial septum/diagonal band complex and spinal cord using two retrograde fluorescent tracers. *Ann NY Acad Sci* 1993; **680**: 462–465.

6. Qu D, Ludwig DS, Gammeltoft S, Piper M, Pelleymounter MA, Cullen MJ, Mathes WF, Przypek R, Kanarek R, Maratos-Flier E. A role for melanin-concentrating hormone in the central regulation of feeding behaviour. *Nature* 1996; **380**: 243–247.

7. Rossi M, Choi SJ, O'Shea D, Miyoshi T, Ghatei MA, Bloom SR. Melanin-concentrating hormone acutely stimulates feeding, but chronic administration has no effect on body weight. *Endocrinology* 1997; **138**: 351–355.

8. Tritos NA, Vicent D, Gillette J, Ludwig DS, Flier ES, Maratos-Flier E. Functional interactions between melanin-concentrating hormone, neuropeptide Y, and anorectic neuropeptides in the rat hypothalamus. *Diabetes* 1998; **47**: 1687–1692.

9. Broberger C, De Lecea L, Sutcliffe JG, Hökfelt T. Hypocretin/orexin- and melanin-concentrating hormone-expressing cells form distinct populations in the rodent lateral hypothalamus: relationship to the neuropeptide Y and agouti gene-related protein systems. *J Comp Neurol* 1998; **28**: 460–474.

10. Drozdz R, Eberle AN. Synthesis and iodination of human [phenylalanine^{13}, tyrosine^{19}] melanin-concentrating hormone for radioreceptor assay. *J Peptide Sci* 1995; **1**: 58–65.

11. Drozdz R, Siegrist W, Baker BI, Chluba-de Tapia J, Eberle AN. Melanin-concentrating hormone binding to mouse melanoma cells *in vitro*. *FEBS Lett* 1995; **359**: 199–202.

12. Scimonelli T, Eberle AN. Photoaffinity labelling of melanoma cell MSH receptors. *FEBS Lett* 1987; **226**: 134–137.

13. Solca F, Siegrist W, Drozdz R, Girard J, Eberle AN. The receptor for *α*-melanotropin of mouse and human melanoma cells. *J Biol Chem* 1989; **264**: 14277–14281.

14. Solca F, Salomon Y, Eberle AN. Heterogeneity of the MSH receptor among B16 murine melanoma subclones. *J Receptor Res* 1991; **11**: 379–390.

15. Fabry M, Schaefer E, Ellis L, Kojro E, Fahrenholz F, Brandenburg D. Detection of a new hormone contact site within the insulin receptor ectodomain by the use of novel photoreactive insulin. *J Biol Chem* 1992; **267**: 8950–8956.

16. Beck-Sickinger AG, Wieland HA, Brunner J. Synthesis, receptor binding, and crosslinking of photoactive analogues of neuropeptide Y. *J Receptor Signal Transduct Res* 1995; **15**: 473–485.

17. Cao YJ, Kojro E, Gimpl G, Jasionowski M, Kasprzykowski F, Lankiewicz L, Fahrenholz F. Photoaffinity labeling analysis of the interaction of pituitary adenylate-cyclase-activating polypeptide (PACAP) with the PACAP type I receptor. *Eur J Biochem* 1997; **244**: 400–406.

18. Bernier SG, Bellemare JM, Escher E, Guillemette G. Characterization of AT4 receptor from bovine aortic endothelium with photosensitive analogues of angiotensin IV. *Biochemistry* 1998; **37**: 4280–4287.

19. Atherton E, Sheppard RC. *Solid Phase Synthesis: a Practical Approach*, IRL Press, Oxford 1989.

20. Eberle AN, Atherton E, Dryland A, Sheppard RC. Peptide synthesis. Part 9. Solid-phase synthesis of melanin concentrating hormone using a continuous-flow polyamide method. *J Chem Soc Perkin I* 1986; 361–367.

21. Kamber B, Hartmann A, Eisler K, Riniker B, Sieber P, Rittel W. The synthesis of cystine peptides by iodine oxidation of S-trityl-cysteine and S-acetamidomethyl-cysteine peptides. *Helv Chim Acta* 1980; **63**: 899–915.

22. Eberle AN, Jäggin Verin V, Solca F, Siegrist W, Kuenlin C, Bagutti C, Stutz S, Girard J. Biologically active mono-iodinated *α*-MSH derivatives for receptor binding studies using human melanoma cells. *J Receptor Res* 1991; **11**: 311–322.

23. Baker BI, Eberle AN, Baumann JB, Siegrist W, Girard J. Effect of melanin concentrating hormone on pigment and adrenal cells *in vitro*. *Peptides* 1985; **6**: 1125–1130.

24. Solca F, Chluba-de Tapia J, Iwata K, Eberle AN. B16-G4F mouse melanoma cells: an MSH receptor-deficient cell clone. *FEBS Lett* 1993; **322**: 177–180.

25. Chluba-de Tapia J, Bagutti C, Cotti R, Eberle AN. Induction of constitutive melanogenesis in amelanotic mouse melanoma cells by transfection of the human melanocortin-1 receptor gene. *J Cell Sci* 1996; **109**: 2023–2030.

26. Siegrist W, Oestreicher M, Stutz S, Girard J, Eberle AN. Radioreceptor assay for *α*-MSH using mouse B16 melanoma cells. *J Receptor Res* 1988; **5**: 323–343.

27. Munson PJ, Rodbard D. Ligand: a versatile computerized approach for characterization of ligand-binding systems. *Anal Biochem* 1980; **107**: 220–239.

28. Eberle AN. Photoaffinity labelling of MSH receptors on *Anolis* melanophores: irradiation technique and MSH photolabels for irreversible stimulation. *J Receptor Res* 1984; **4**: 315–329.

29. Herblin WF, Kauer JC, Tam SW. Photoinactivation of the *μ* opioid receptor using a novel synthetic morphiceptin analog. *Eur J Pharmacol* 1987; **139**: 273–279.

30. Boyd ND, White CF, Cerpa R, Kaiser ET, Leeman SE. Photoaffinity labeling the substance P receptor using a derivative of substance P containing *p*-benzoylphenylalanine. *Biochemistry* 1991; **30**: 336–342.

31. McNicoll N, Escher E, Wilkes BC, Schiller PW, Ong H, De Lean A. Highly efficient photoaffinity labeling of the hormone binding domain of atrial natriuretic factor receptor. *Biochemistry* 1992; **31**: 4487–4493.

32. Shoelson SE, Lee J, Lynch CS, Baker JM, Pilch PF. BpaB25 insulins. Photoactivatable analogues that quantiatively cross-link, radiolabel, and activate the insulin receptor. *J Biol Chem* 1993; **268**: 4085–4091.

33. Schumann C, Steinmetzer T, Gothe R, Hoppe A, Paegelow I, Liebmann C, Fabry M, Brandenburg D, Reissmann S. *Biol Chem Hoppe Seyler* 1995; **376**: 33–38.

34. Servant G, Laporte SA, Leduc R, Escher E, Guillemette G. Identification of angiotensin II-binding domains in the rat AT2 receptor with photolabile angiotensin analogs. *J Biol Chem* 1997; **272**: 8653–8659.

35. Bisello A, Adams AE, Mierke DF, Pellegrini M, Rosenblatt M, Suva LJ, Chorev M. Parathyroid hormone-receptor interactions identified directly by photocrosslinking and molecular modeling studies. *J Biol Chem* 1998; **273**: 22498–22505.

36. Abe T, Nishiyama K, Snajdar R, He X, Misono KS. Aortic smooth muscle contains guanylate-cyclase-coupled 130-kDa atrial natriuretic factor receptor as predominant receptor form. Spontaneous switching to 60-kDa C-receptor upon cell culturing. *Eur J Biochem* 1993; **217**: 295–304.